

## Evaluation of Temperature Dependent Models for PV Yield Prediction

Wei Liao<sup>1</sup>, Yeonsook Heo<sup>1</sup>, Shen Xu<sup>2</sup>

<sup>1</sup>Department of Architecture, University of Cambridge, Cambridge CB2 1PX, United Kingdom

<sup>2</sup>School of Architecture, Huazhong University of Science and Technology, 430074, China

### Abstract

This paper investigated temperature-dependent models in predicting PV yield. Seven different models based on different approaches (i.e., constant temperature, physics-based and statistical methods) are summarized and compared through a case study of Wuhan area in China. The case study shows the limitations of using the constant temperature approaches. The case study reveals that a constant PV cell temperature specified in NOCT is much higher than those predicted by the non-constant methods for all walls and roofs in the studied area. As a result, NOCT substantially underpredicts the PV yield. Another constant temperature model, STC, yields the PV power prediction in good agreement with the non-constant methods but over-predicts the PV power during the summer time. The case study also shows significant difference in the PV cell temperature prediction due to the choice of the model, but relatively smaller impacts on the PV output power.

### Introduction

In recent years, interest in utilising solar potential in urban areas has been rising. Many solar map products of different cities or regions have been developed to provide information about received solar energy distributed over the area in terms of irradiance amount (kWh/m<sup>2</sup>) or intensity (W/m<sup>2</sup>) on building roofs and building facades. These solar maps show the results of daylight simulation that uses GIS data and historical weather data as inputs to predict solar potential for a whole urban area. Prediction of solar potential has been performed to evaluate planning policies and guidelines with respect to their effect on solar availability (Kanters and Wall, 2016) and quantify the impact of new urban developments on the performance of existing solar collectors (Zomer and R  ther, 2017). Prediction of solar irradiance is also a necessary step to identify the most solar-potential locations in the urban fabric for solar collectors.

In addition to solar irradiance prediction, PV system model is necessary to predict energy generation. PV system converts solar energy into electricity, but conversion efficiency decreases when PV cell operating temperature rises. Existing research found that different PV operating temperatures affected the amount of PV yield as much as 30% (Radziemska, 2003). In order to improve the prediction accuracy, latest improvement

was made in PV yield models to incorporate the temperature dependence of PV performance. A key element for prediction of PV yield is predicting PV cell operating temperature that impacts PV system efficiency. Different models, ranging from high-fidelity physics-based models to simplified models, have been developed to predict PV cell operating temperature (Skoplaki et al., 2009; Dubey et al., 2013). Existing models can be grouped into three types: (1) constant temperature models, (2) physics-based models, and (3) statistical models. Constant temperature methods simply use a constant value of PV cell operating temperature to determine the PV yield regardless of weather and PV working conditions. Physics-based methods are the most studied in the field with large number of established models. These models are based on a simplified form of the physical model and include correlation coefficients that capture the effect of key physical variables to simplify certain parts of the physical model. Many of them correlated PV module temperature as a function of diode PV model electronic parameters: resistance, current, voltage, and band gap (Yordanov et al., 2012) and system-dependent properties such as glazing-cover transmittance and plate absorptance (Skoplaki et al., 2009). Statistical models, on the other hand, require much less inputs as they are typically based on the simplest mathematical equation, often derived from the physical model and derive unknown model coefficients by fitting the model to the measured PV yield data. Some of the latest statistical models also use artificial intelligent methods to predict the temperature. Further discussion of these models and methods will be provided in the next section. Existing study has been looking into the impact of temperature dependent model at national level and found a maximum of 20% difference of PV yield given different locations and season in the U.S. (Bayrakci et al., 2013).

The paper aims to investigate the effect of different temperature-dependent models on the PV cell temperature and PV yield prediction for solar analysis of building surfaces in urban environments. An urban area in Wuhan, China is used as a case study to predict solar irradiance distributed over the urban fabric and compare PV cell operating temperature and PV yield predictions computed by different models.

## Existing PV cell operating temperature models

Before investigating different PV cell operating temperature models, it is worth describing the role of PV cell operating temperature in computing the PV output power as defined in the equation (1):

$$P = G_T \beta_{ref} (1 + \eta_{ref}(T_c - T_{ref})) \quad (1)$$

$G_T$  is the received solar irradiance,  $\beta_{ref}$  is the PV conversion rate under the reference (STC) temperature ( $T_{ref} = 25^\circ\text{C}$ ).  $\eta_{ref}$  is the temperature coefficient of the PV module. Common values for  $\beta_{ref}$  and  $\eta_{ref}$  are summarised in Table 1,  $T_c$  is the PV cell operating temperature calculated by the models compared in this study.

Table 1: PV module properties

	$T_{ref}$	$\eta_{ref}$
polycrystalline-silicon PV	13.0%	-0.48 %
amorphous-silicon PV	5.5%	-0.20%

\*Values provided through a survey by HOMER (2017)

Table 2 lists three different sets of methods developed to predict PV cell operating temperature  $T_c$ . In total, seven methods are summarised in the table and grouped into three types in terms of their mathematical formulation and input requirements. The performance of the listed methods will be investigated through a case study in the latter section.

Table 2: Existing models and methods

Type	Model	Reference
Constant temperature	STC	(Munoz et al., 2011)
	NOCT	(Koehl et al., 2011)
Physics-based	Skoplaki's model (a)	(Skoplaki et al., 2008)
	HOMER model	(HOMER, 2017)
	Empirical Ross coefficient method	(Ross, 1976)
Statistical	Skoplaki's model (b)	(Skoplaki et al., 2008)
	Muzathik's model	(Muzathik, 2014)

### Constant temperature

Constant temperature methods assume the PV module operates at a fixed temperature all the time regardless of weather conditions and dynamic PV working conditions. Hence, using constant temperature models always yields a fixed PV conversion rate throughout the year. This type of methods may be useful when one requires a quick estimation of PV yield. The most commonly used temperatures are standard test condition temperature (STC) and nominal operating cell temperature (NOCT).

Standard test conditions are specific laboratory conditions that represent peak sunshine on a surface directly facing the sun in a day without clouds. PV modules are tested under STC as follows: irradiance of  $1000\text{W/m}^2$ ; a surface temperature of  $25^\circ\text{C}$ ; a light spectrum that closely simulates sunlight; air mass at 1.5G given a standard temperature and water vapour content (Munoz et al., 2011). These are idealized conditions, which does not reflect the real PV system

operation conditions. Indeed, often, PV systems operate at higher temperatures than STC due to the heat received from the sunlight and high ambient temperature.

A new test standard NOCT was established to reflect the real PV operation conditions. In NOCT, the assumed irradiance is  $800\text{W/m}^2$ , which takes into account the fact that PV modules don't always face the sun. It also considers atmospheric or geographic conditions what might diminish sunshine. Heat convection is also considered with a wind speed of  $1\text{ m/s}$  at  $20^\circ\text{C}$  ambient temperature (Koehl et al., 2011). Under this condition, the measured cell temperature of a certain PV module is then defined as NOCT. PV manufacturers typically report the NOCT of their products as part of manufacturer's catalogues. One survey of commercially-available PV modules in 2007 summarised that about 60% of the PV products have NOCT values ranging from  $45^\circ\text{C}$  to  $48^\circ\text{C}$  (HOMER, 2017). A medium value of  $46.5^\circ\text{C}$  is assigned as NOCT in our case study for comparison of different models.

Although NOCT was developed to reflect more realistic PV cell operating temperature than STC temperature, it ignores actual dynamic weather conditions such as solar radiation and ambient temperature and, as a result, undermines the predication accuracy under dynamic weather conditions that vary from the assumed standard conditions. A study measured the PV cell operating temperatures of four different types of insulated PV panels for 9 months in Gaithersburg, Maryland, and revealed the unsuitability of using NOCT to predict the PV cell operating temperature under varied irradiance conditions as shown in Figure 1. (Davis et al., 2002). NOCT did not represent the dynamic behaviour of PV systems, and the discrepancy between NOCT and measured temperatures was up to  $20^\circ\text{C}$ . Nonetheless, the constant temperature methods are still commonly used in the industry to estimate PV yield.

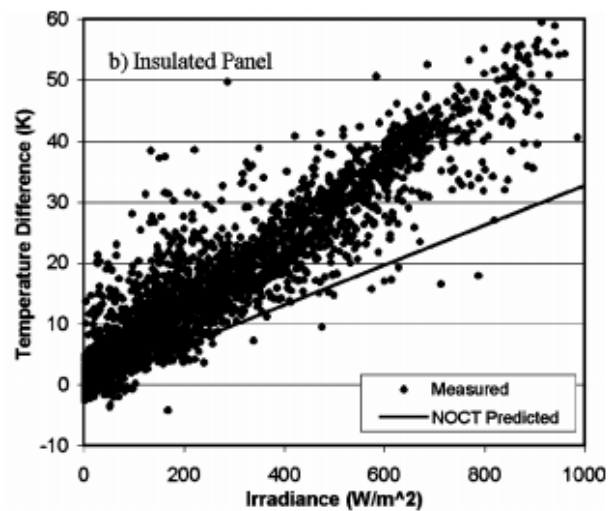


Figure 1: Temperature difference using NOCT compared to measurements. (Davis et al., 2002)

## Physics-based methods

Physics-based models have been developed to compute dynamic PV operating cell temperatures. For a detailed analysis of PV systems, high-fidelity dynamic simulation models have been used to accurately predict PV surface temperatures (Lobera and Valkealahti, 2013). However, for urban-scale analysis, we believe relatively simple physics-based models are more suitable given the scale of analysis and limited data about individual buildings. Thus, two simplified physics-based models on the basis of the steady-state energy balance concept were investigated.

Skoplaki et al. (2008) developed a physics-based algorithm to calculate actual PV cell operating temperatures in relation to NOCT that is measured and provided by the manufacturers' catalogues. They developed the formula below, adopted by many studies, that predict PV cell operating temperatures on the basis of physical properties of the cell and weather conditions (i.e., ambient temperature, solar irradiance, and wind speed):

$$T_c = \frac{T_a + \left(\frac{G_T}{G_{NOCT}}\right) \frac{h_w^{NOCT}}{h_w} (T_{NOCT} - T_{a,NOCT}) [1 - \frac{\eta_{nef}}{\tau \alpha} (1 + \beta_{nef} T_{ref})]}{1 - \frac{\beta_{nef} T_{ref}}{\tau \alpha} \left(\frac{G_T}{G_{NOCT}}\right) \left(\frac{h_w^{NOCT}}{h_w}\right) (T_{NOCT} - T_{a,NOCT})} \quad (2)$$

GNOCT and  $T_{a,NOCT}$  denote standard settings used to measure NOCT; the first refers to the irradiance of 800W/m<sup>2</sup>, and the latter refers to the ambient temperature of 20°C.  $T_{a,NOCT}$  indicates NOCT (46.5 °C used in the case study). The solar transmittance of the PV panel is denoted as  $\tau$ , and the solar absorptance of the panel is denoted as  $\alpha$ .  $\alpha \times \tau$  value is commonly assumed to be 0.9 (Duffie and Beckman, 1991).  $G_T$  indicates the magnitude of solar irradiance on the PV panel, which can be obtained by daylight simulation or provided by existing solar maps. Ambient temperature  $T_a$  is obtained from publicly available hourly weather data, but using this data assumes that ambient temperature in the entire urban area is the same.  $h_w$  indicates convective heat transfer coefficient, which heavily depends on the wind speed. Among a wide range of convective heat transfer coefficient equations in the literature (Palyvos, 2008), Skoplaki et al. (2008) used a linear regression model that correlates the coefficient to wind speed (Loveday and Taki, 1996) as below:

$$h_w = 8.91 + 2.0V_f \quad (3)$$

Where  $V_f$  is the free stream wind speed. Similar to the ambient temperature, publicly available wind speed data for the meteorological region corresponding to the case study area is used for the entire urban area. Hence, the equation (1) only captures the effect of regional weather conditions on the PV performance, but does not present different PV performances within the urban area due to varying microclimate conditions.

Another model, simplified from the formula above, was developed by Duffie and Beckman (1991) as defined in (4). The model assumes the same convective heat transfer coefficient as the nominal conditions throughout

the year. Except this assumption, the formula is almost identical to the Skoplaki's model, and presents the effect of the PV system characteristics, solar irradiance, and ambient temperature on the PV operating temperature. Further description of the model is provided in (HOMER, 2017).

$$T_c = \frac{T_a + \left(\frac{G_T}{G_{NOCT}}\right) (T_{NOCT} - T_{a,NOCT}) [1 - \frac{\eta_{nef}}{\tau \alpha} (1 + \beta_{nef} T_{ref})]}{1 - \frac{\beta_{nef} T_{ref}}{\tau \alpha} \left(\frac{G_T}{G_{NOCT}}\right) (T_{NOCT} - T_{a,NOCT})} \quad (4)$$

The third chosen model is a semi-empirical model with a Ross coefficient:

$$T_c = T_a + kG_T \quad (5)$$

In this linear expression, the Ross coefficient  $k$  expresses temperature rises above the ambient temperature due to the increasing solar flux (Ross, 1976):

$$k = \Delta(T_c - T_a) / \Delta G_T \quad (6)$$

The Ross coefficient value suggested by existing studies ranges between 0.02–0.04 K·m<sup>2</sup>/W (Buresch, 1983; Ross, 1976). An IEA study provides standard Ross coefficient values depending on the level of integration and mounting types (Nordmann and Clavadetscher, 2003). Table 3 lists typical coefficient values for different mounting types provided by the IEA study.

Table 3: Standard values of the Ross coefficient  $k$  for various mounting types

PV array mounting type	$k$ (K·m <sup>2</sup> /W)
Free standing	0.021
Flat roof	0.026
Sloped roof: well cooled	0.020
Sloped roof: not so well cooled	0.034
Sloped roof: highly integrated, poorly ventilated	0.056
Facade integrated: transparent PV	0.046
Facade integrated: opaque PVs	0.054

The Ross coefficient values in Table 3 are used in our case study with scenarios of varying mounting types.

## Statistical models

In general, existing statistical models can be categorised into two types: artificial intelligence methods and linear models. Artificial intelligence methods include artificial neural networks (Ceylan et al., 2014) or adaptive neuro Fuzzy inference system (Bassam et al., 2017). The main advantages of these methods are their versatility to capture complex trends, but as they are black-box models, they do not explicitly show relationships between explanatory variables and dependent variable. Linear models, on the other hand, are the simplest approach that captures linear trends between the key environmental variables and PV cell operating temperature.

Two statistical models were chosen in this paper for comparison. The first one is the Skoplaki's semi-empirical model, simplified version of the formula (1):

$$T_c = T_a + \left( \frac{0.32}{8.91 + 2.0V_f} \right) G_T \quad (7)$$

The formula correlates the PV cell operating temperature to the three environmental variables: ambient temperature ( $T_a$ ), free-stream wind speed ( $V_f$ ), and solar irradiance received on the PV cell ( $G_T$ ). The temperature estimated by the model showed a difference of less than 3 °C in comparison to its original formula (1) (Skoplaki et al., 2008). However, as this statistical model was derived on the basis of the data collected from free-standing PV systems, its applicability to other forms of PV mounting needs to be investigated.

The second statistical model chosen in this study is Muzathik's model (Muzathik, 2014):

$$T_c = 0.943T_a + 0.0195G_T - 1.528V_f + 0.3529 \quad (8)$$

The model correlates  $T_c$  with the same set of three environmental variables. It was developed by fitting a linear regression model to measured data from a polycrystalline silicon PV module mounted on the wooden frame on a flat roof in Malaysia. This model was demonstrated to show less than 1.5 °C difference compared to measurements (Muzathik, 2014). However, unlike the semi-empirical models, the performance of the linear regression model without explicit expression of underlying physics highly relies on the training data used for model development. Hence, the applicability of the linear model to other climate conditions needs to be tested.

## Case study

We compare the performance of the chosen methods through a case study of Wuhan urban area in which all building surfaces are assumed to be implemented with PV modules to achieve the maximum solar potential of the entire urban area. A 0.72 km<sup>2</sup> city area (1.2 km × 0.6 km) located in Hankou district in Wuhan, China was selected as a case study. Urban geometry in the studied area, including building roofs and ground surfaces (Figure 2), was assumed to be flat as Wuhan is located in plain region and slope roofs or curved envelopes are not common in the chosen area. A window to wall ratio of 0.3 was given to all buildings in the studied urban area. Solar irradiance of all surfaces was calculated by the simplified method recently developed by Liao and Heo (2017), which was validated against the advanced daylight simulation software (Radiance). 10m × 10m mesh grid was applied to each of the building surfaces, and the calculated irradiance of each mesh represents the received irradiance of PV modules located in the corresponding surface.

In this study, we considered two types of PV systems: polycrystalline-silicon PV systems for opaque roofs and walls and amorphous-silicon PV systems for transparent windows. Since the Ross method requires the information of PV mounting types, we assumed that half of roofs are equipped with free standing PV modules, the other half with flat roof PV modules, all walls with opaque PV modules, and all windows with transparent

PV modules. PV electricity yield was calculated using the formula (1).

In the case study, the different methods are compared in terms of the PV cell temperature and PV yield at different time resolution scales: solar peak time (noon) and monthly scale.

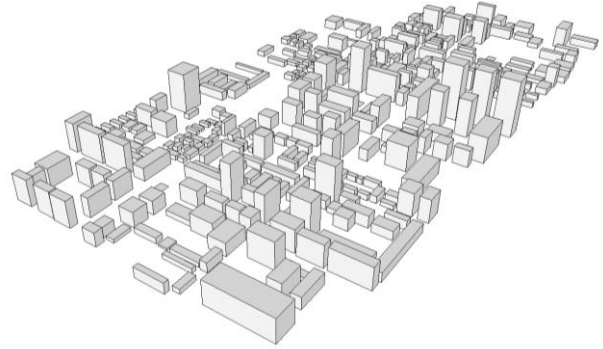


Figure 2: Illustration of the urban geometry

## Results

Figure 3 shows the average irradiance at noon throughout the year (365 noons) for individual roofs and walls. The noon time represents the peak solar irradiance, which is used as standard test conditions for constant temperature models. The standard solar intensity conditions (i.e., 1000 W/m<sup>2</sup> for STC and 800 W/m<sup>2</sup> for NOCT) are far higher than the range of solar radiation for roofs and walls in the studied urban area. More interestingly, the urban shading caused by surrounding buildings result in wide variation in the received irradiance for both roofs and walls. Especially for walls, received irradiances vary from 50W/m<sup>2</sup> to 400W/m<sup>2</sup>. Differences in the received irradiance for roofs are relatively smaller since roofs are usually less shaded than walls.

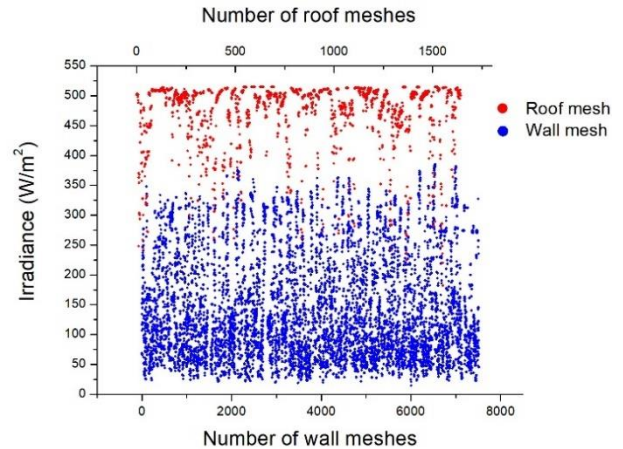


Figure 3: Average irradiance on all roofs and walls at noon

Given these various irradiance conditions, we calculated the PV cell temperature using the seven methods. Figure 4 shows the box plot of PV cell temperature of all building surfaces at noon time, calculated by among the different methods. Results show that NOCT is much

higher than all the other predictions while STC is close to the average temperatures (denoted as \*) calculated by the non-constant methods. Among the non-constant methods, Empirical Ross computes the highest value with an average of 28.2 °C, followed by HOMER ( $T_c=25.9^\circ\text{C}$ ) and Skoplaki's (b) ( $T_c=24.7^\circ\text{C}$ ). Muzathik linear model yields much lower values ( $T_c=18.72^\circ\text{C}$ ) than the other methods. This may be due to the inability of the statistical model to extrapolate from the Malaysia weather data used for model development to Wuhan weather conditions. In addition, significant differences are observed in the range of PV cell temperatures predicted by the non-constant methods. Empirical Ross method results in a difference of 20 °C in the PV cell temperature whereas the other methods results in a difference of around 10 °C. Since the same hour data of ambient temperature and wind speed is used for the entire studied area, differences in the predicted PV cell temperature at noon time are due to the differences in the received solar intensity as a result of different orientations and mutual shading conditions. However, for monthly and yearly predictions, the temporal variation in the ambient temperature and wind speed can be accounted for in prediction of the cell temperature depending on the choice of the model.

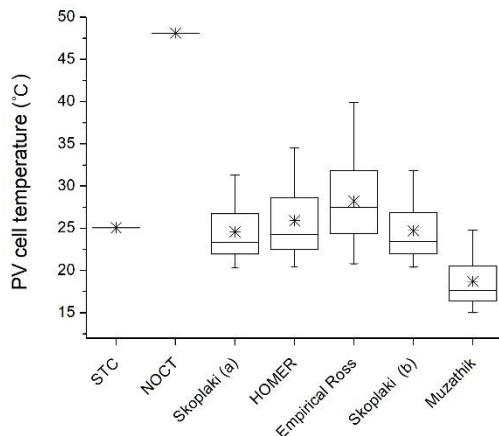


Figure 4: predicted PV cell operation temperature of all urban surfaces at noon

As roofs and walls receive quite different levels of irradiance, we closely looked into the performance of the different methods separately for roofs and walls. PV cell temperature predictions at noon time for the roofs are shown in Figure 5. All the non-constant methods except Muzathik method yields cell temperatures approximately 5 to 10 C° higher than STC, but still much lower than NOCT. For the roofs, the variation in the cell temperature is very small (around 3 °C). The differences in the average PV cell temperature predicted by the non-constant methods are also very small. The prediction results for the walls are shown in Figure 6. As the walls take up more than 70% of the total surfaces, the predictions of the PV cell temperature for the walls are quite similar to the overall results. A significant variation in the PV cell temperature is observed for the walls due

to shading effects of surrounding buildings in urban environments. In addition, Empirical Ross method results in a much wider range of the cell temperature predictions than the other methods as it uses a different coefficient depending on the PV mounting type. In general, STC seems a reasonable value used to predict PV peak yield for walls, but for roofs, neither STC nor NOCT reflects the results calculated by the non-constant models.

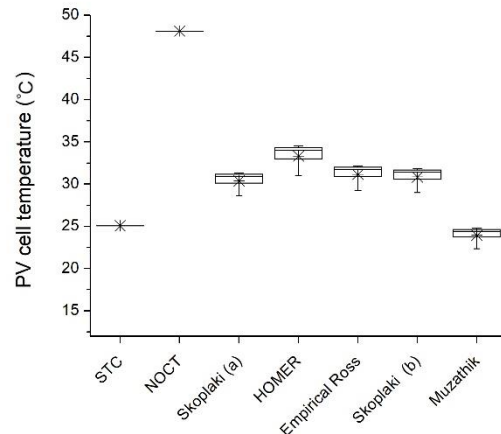


Figure 5: predicted PV cell temperatures of roofs at noon

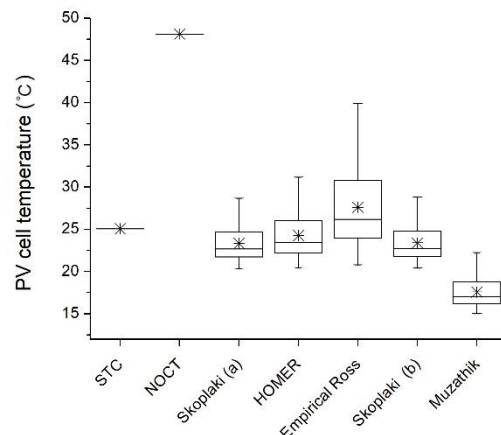


Figure 6: predicted PV cell temperatures of walls at noon

We have so far compared the methods in terms of their predictions for the peak irradiance period. However, one of key performance indicators used for urban-scale solar analysis is the total PV yield throughout the year. Hence, monthly PV cell temperature and PV output power are used for further analysis. Figures 7 and 8 illustrate the monthly average PV cell operating temperature predictions during day time. The pattern of monthly temperature variations is quite similar between roofs and walls. However, the cell temperatures for roofs are constantly higher (2 - 8°C) than those for walls. The magnitude of differences in the temperature prediction between different methods for both walls and roofs is similar: approximately 7 °C and 10 °C difference for the

summer and winter, respectively. In general, differences in the monthly prediction by the non-constant methods are much larger than the peak-time prediction. This is expected as solar radiation intensity, ambient temperature, and wind speed substantially vary depending on the season, and the non-constant models have a different formula to incorporate their effect on the cell temperature. Except Muzathik's method, all temperature-dependent methods compute similar PV cell operating temperature predictions. Muzathik's method computes lower temperatures than the other methods, which are even lower than the ambient temperature. PV cell operating temperature is very unlikely to be below ambient temperature during day time due to solar heat gains. As Muzathik's method is a linear regression model based on the hot climate data, it does not properly predict the cell temperature for other locations with milder climate conditions.

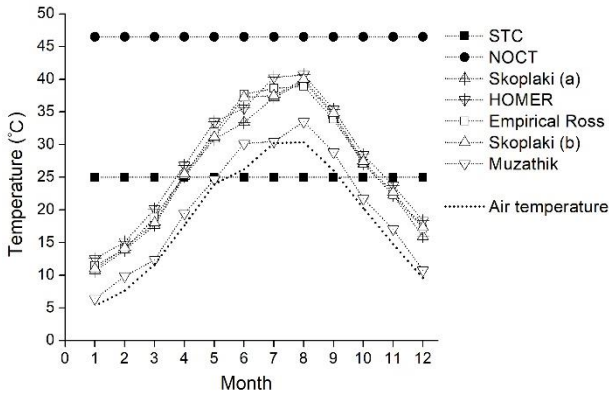


Figure 7: Monthly average PV cell temperatures for roofs

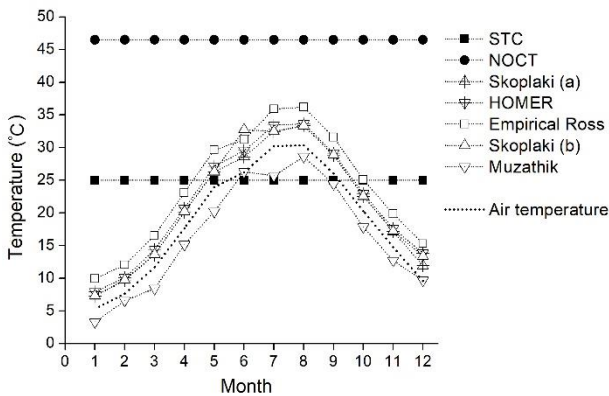


Figure 8: Monthly average PV cell temperatures for walls

Figures 9 and 10 illustrate the predicted monthly average PV output powers ( $W/m^2$ ) for roofs and walls, respectively. It is obvious that PV power outputs for roofs are a lot higher than for walls if we assume all walls, including heavily shaded ones, are implemented with PV. However, it does not mean that walls are not

suitable for PV applications as we can also clearly see in Figure 3 that a considerable number of walls receive sufficient irradiance. This suggests that the solar potentials of walls should be carefully examined with consideration of the mutual shading for selection of wall areas and design of PV systems. Owing to the low average irradiance on walls, different methods do show a very little difference in the PV power prediction. However, for roof predictions, they result in the difference, ranging between 4 to 10  $W/m^2$ . In general, STC yields PV power predictions close to the non-constant methods except the summer season where STC prediction is higher than the others. As NOCT uses the much higher cell temperature than the non-constant methods, it substantially under-predicts the PV yield in comparison to the non-constant methods. Differences in the PV power predicted by the different non-constant methods are approximately between 1 - 4  $W/m^2$ . The differences are smaller during the winter than during the summer.

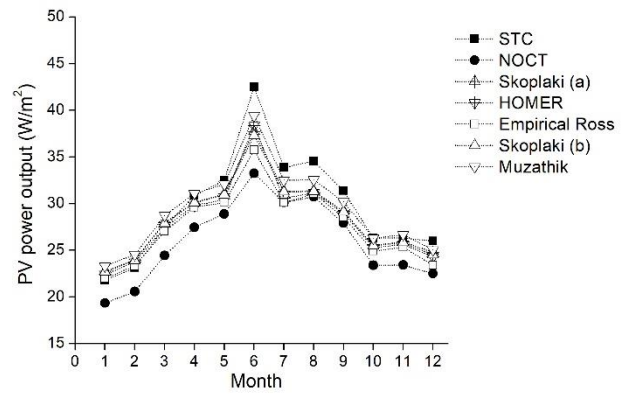


Figure 9: Monthly average PV yields for roofs

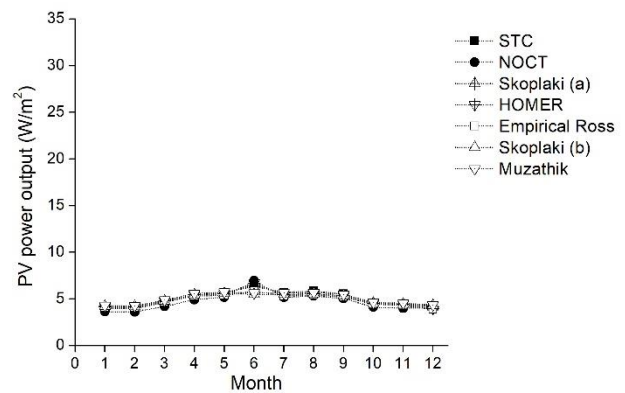


Figure 10: Monthly average PV yields for walls

## Conclusion

This paper investigated the value of incorporating temperature-dependent models in predicting PV yield at urban scale by comparing the existing PV cell operating temperature models through a case study of Wuhan area

in China. Seven different models (i.e., constant temperature, physics-based, and statistical methods) were compared in terms of the PV cell operating temperature and PV electricity yield prediction. On the one hand, STC yields the monthly PV power prediction in good agreement with the non-constant methods but over-predicts the monthly PV power during the summer time. On the other hand, as NOCT is much higher than PV cell temperatures predicted by the non-constant methods, it substantially under-predicts the monthly PV yield throughout the year. The non-constant methods result in the quite similar results except Muzathik's method, which highlights the usefulness of maintaining underlying physics in a simplified empirical model. The case study shows relatively significant differences in the PV cell temperature prediction but smaller impacts on the PV output power.

This paper is part of an on-going research project with aim to develop the whole analysis package for urban-scale evaluation of solar potentials in urban environments. In addition to a simplified method already developed for urban-scale irradiance prediction (Liao and Heo, 2017), this paper provides a detailed comparison of different methods in terms of the PV cell temperature and PV yield. This comparison helps modellers make a well-informed decision about the PV system model by investigating the value of using more sophisticated methods such as physic-based models in comparison to constant temperatures. As the next step, a case study with varying design scenarios will be performed to evaluate the relevance of different levels of modelling methods, including irradiation models and PV system models, in design of urban-scale policy strategies or solar technologies.

## Nomenclature

$V_f$	free stream wind speed, m/s
$T_{NOCT}$	Nominal Operating Cell Temperature, °C
$T_c$	PV cell operating temperature, °C
$T_{a,NOCT}$	ambient temperature under NOCT test condition, °C
$T_a$	ambient temperature, °C
$k$	Ross coefficient
$h_{w,NOCT}$	wind-convection heat transfer coefficient under NOCT wind speed (1m/s) condition, W/m <sup>2</sup> K
$h_w$	wind-convection heat transfer coefficient, W/m <sup>2</sup> K
$G_{T,NOCT}$	solar irradiance under NOCT test condition, (800W/m <sup>2</sup> )
$G_T$	received solar irradiance, W/m <sup>2</sup>
$\alpha$	solar absorptance
$\beta_{ref}$	PV conversion rate at 25 °C
$\eta_{ref}$	PV temperature coefficient
$\tau$	solar transmittance

## Acknowledgement

This work is supported by the Natural Science Foundation of China under the Contract No. 51678261 and the CSC Cambridge International Scholarship.

## References

- Bassam, A., May Tzuc, O., Escalante Soberanis, M., Ricalde, L. J., & Cruz, B. (2017). Temperature Estimation for Photovoltaic Array Using an Adaptive Neuro Fuzzy Inference System. *Sustainability* 9(8), 1399.
- Bayrakci, M., Choi, Y., & Brownson, J. R. (2014). Temperature dependent power modeling of photovoltaics. *Energy Procedia* 57, 745-754.
- Buresch M. (1983). Photovoltaic energy systems: Design and installation.
- Ceylan, İ., Erkamaz, O., Gedik, E., & Gürel, A. E. (2014). The prediction of photovoltaic module temperature with artificial neural networks. *Case Studies in Thermal Engineering* 3, 11-20.
- Davis, M. W., Fannery, A. H., & Dougherty, B. P. (2001). Prediction of building integrated photovoltaic cell temperatures. *Journal of Solar Energy Engineering* 123(3), 200-210.
- Dubey, S., Sarvaiya, J. N., & Seshadri, B. (2013). Temperature dependent photovoltaic (PV) efficiency and its effect on PV production in the world—a review. *Energy Procedia* 33, 311-321.
- Duffie JA, Beckman WA. (1991). *Solar Engineering of Thermal Processes 2nd edition*, Wiley, New York, NY
- HOMER (2017). <https://www.homerenergy.com>.
- Kanters J, Wall M. (2016). A planning process map for solar buildings in urban environments. *Renewable and Sustainable Energy Reviews* 57,173-185.
- Koehl, M., Heck, M., Wiesmeier, S., & Wirth, J. (2011). Modeling of the nominal operating cell temperature based on outdoor weathering. *Solar Energy Materials and Solar Cells* 95(7), 1638-1646.
- Liao, W., Heo, Y. (2017). A simplified method for irradiance prediction in urban environments. *15<sup>th</sup> Building simulation conference*.
- Loveday, D. L., & Taki, A. H. (1996). Convective heat transfer coefficients at a plane surface on a full-scale building facade. *International Journal of Heat and Mass Transfer* 39(8), 1729-1742.
- Lobera, D. T., & Valkealahti, S. (2013). Dynamic thermal model of solar PV systems under varying climatic conditions. *Solar energy* 93, 183-194.
- Munoz, M. A., Alonso-García, M. C., Vela, N., & Chenlo, F. (2011). Early degradation of silicon PV modules and guaranty conditions. *Solar energy* 85(9), 2264-2274.

- Muzathik, A. M. (2014). Photovoltaic modules operating temperature estimation using a simple correlation. *International Journal of Energy Engineering* 4(4), 151.
- Nordmann, T., & Clavadetscher, L. (2003, May). Understanding temperature effects on PV system performance. In *Photovoltaic Energy Conversion, 2003. Proceedings of 3rd World Conference on* (Vol. 3, pp. 2243-2246). IEEE.
- Palyvos, J. A. (2008). A survey of wind convection coefficient correlations for building envelope energy systems' modeling. *Applied Thermal Engineering* 28(8-9), 801-808.
- Patel, H., & Agarwal, V. (2008). MATLAB-based modeling to study the effects of partial shading on PV array characteristics. *IEEE transactions on energy conversion* 23(1), 302-310.
- Radziemska, E. (2003). The effect of temperature on the power drop in crystalline silicon solar cells. *Renewable energy* 28(1), 1-12.
- Robinson, D., & Stone, A. (2004). Solar radiation modelling in the urban context. *Solar energy* 77(3), 295-309.
- Ross Jr, R. G. (1976). Interface design considerations for terrestrial solar cell modules. In *12th Photovoltaic Specialists Conference*, 801-806.
- Sera, D., & Baghzouz, Y. (2008, October). On the impact of partial shading on PV output power. In *WSEAS/IASME International Conference on Renewable Energy Sources*, 229-234.
- Skoplaki, E., Boudouvis, A. G., & Palyvos, J. A. (2008). A simple correlation for the operating temperature of photovoltaic modules of arbitrary mounting. *Solar Energy Materials and Solar Cells* 92(11), 1393-1402.
- Skoplaki, E., & Palyvos, J. A. (2009). On the temperature dependence of photovoltaic module electrical performance: A review of efficiency/power correlations. *Solar energy* 83(5), 614-624.
- Salam, Z., Ahmed, J., & Merugu, B. S. (2013). The application of soft computing methods for MPPT of PV system: A technological and status review. *Applied Energy* 107, 135-148.
- Yordanov, G. H., Midtgård, O. M., & Saetre, T. O. (2012). Series resistance determination and further characterization of c-Si PV modules. *Renewable Energy* 46, 72-80.
- Zomer, C., & Rüther, R. (2017). Simplified method for shading-loss analysis in BIPV systems—part 1: Theoretical study. *Energy and Buildings* 141, 69-82.